The role of the spatial resolution of a three-dimensional hydrodynamic model for marine transport risk assessment*

OCEANOLOGIA, 53 (1-TI), 2011.
pp. 309–334.

KEYWORDS
Ocean modelling
Environmental risks
Risk modelling
Gulf of Finland
Baltic Sea
Pollution propagation
Maritime spatial planning

Oleg Andrejev[1]
Tarmo Soomere[2,⋆]
Alexander Sokolov[3]
Kai Myrberg[1]

[1] Finnish Environment Institute,
Marine Research Centre,
P.O. Box 140, Helsinki 00251, Finland

[2] Institute of Cybernetics,
Tallinn University of Technology,
Akadeemia tee 21, Tallinn 12618, Estonia;

e-mail: soomere@cs.ioc.ee

⋆corresponding author

[3] Baltic Nest Institute,
Stockholm Resilience Centre,
Stockholm University,
Stockholm 10691, Sweden

Received 6 October 2010, revised 31 January 2011, accepted 5 February 2011.

* This study was supported by funding from the European Community's Seventh Framework Programme (FP/2007–2013) under grant agreement No. 217246 made with the joint Baltic Sea research and development programme BONUS for the BalticWay project, which attempts to reduce the risk of vulnerable sea areas being polluted by placing potentially dangerous activities in specific offshore regions. The research was partially supported by targeted financing from the Estonian Ministry of Education and Science (grants SF0140077s08 and SF0140007s11) and the Estonian Science Foundation (grant No. 7413).

Abstract

The paper addresses the sensitivity of a novel method for quantifying the environmental risks associated with the current-driven transport of adverse impacts released from offshore sources (e.g. ship traffic) with respect to the spatial resolution of the underlying hydrodynamic model. The risk is evaluated as the probability of particles released in different sea areas hitting the coast and in terms of the time after which the hit occurs (particle age) on the basis of a statistical analysis of large sets of 10-day long Lagrangian trajectories calculated for 1987–1991 for the Gulf of Finland, the Baltic Sea. The relevant 2D maps are calculated using the OAAS model with spatial resolutions of 2, 1 and 0.5 nautical miles (nm) and with identical initial, boundary and forcing conditions from the Rossby Centre 3D hydrodynamic model (RCO, Swedish Meteorological and Hydrological Institute). The spatially averaged values of the probability and particle age display hardly any dependence on the resolution. They both reach almost identical stationary levels (0.67–0.69 and ca 5.3 days respectively) after a few years of simulations. Also, the spatial distributions of the relevant fields are qualitatively similar for all resolutions. In contrast, the optimum locations for fairways depend substantially on the resolution, whereas the results for the 2 nm model differ considerably from those obtained using finer-resolution models. It is concluded that eddy-permitting models with a grid step exceeding half the local baroclinic Rossby radius are suitable for a quick check of whether or not any potential gain from this method is feasible, whereas higher-resolution simulations with eddy-resolving models are necessary for detailed planning. The asymptotic values of the average probability and particle age are suggested as an indicator of the potential gain from the method in question and also as a new measure of the vulnerability of the nearshore of water bodies to offshore traffic accidents.

1. Introduction

Comprehensive progress in the environmental management of anthropogenic pressure on particularly vulnerable sea areas, such as the Baltic Sea (Kachel 2008), has now become feasible as a result of major advances in marine sciences leading to a rapid increase in the accuracy with which the current-driven transport of adverse impacts is represented. These advances comprise computational facilities, high-resolution circulation modelling, new technologies for in situ and satellite observations, an ever increasing flow of real-time information about the sea state, increasing experience in operational oceanography (including oil spill monitoring and forecasting), and increasingly accurate meteorological forecasts (Leppäranta & Myrberg 2009).

While a number of studies address environmental issues in terms of the Lagrangian transport of different adverse impacts (see Havens et al. 2010 and the references therein), very few attempts have been targeted at the preventive reduction of environmental risks caused by maritime industry and

transport. Among these are the system of the dynamic relocation of tugboats along the Norwegian Atlantic coast (Lehmann & Sørgård 2000) and the underlying models of dynamic risk (Eide et al. 2007). Preventive methods usually require the solution of an inverse problem for the propagation of the adverse impact. Mathematically, this is often very demanding. Also, the details of the hydrodynamic patterns necessary for an accurate treatment of inverse problems are extremely difficult to reproduce, not only because of the considerable computational expense but also because of the uncertainties intrinsic to external forcing and the initial and boundary conditions.

A feasible way of finding approximate solutions to inverse problems of this type is to use advanced statistical methods to analyse a large number of particular solutions to the direct problem of current-driven transport. A method for quantifying the potential of offshore areas to be a source of danger to coastal regions, based on the above idea, has recently been developed by Soomere et al. (2010, 2011b). In many cases, solutions have been found using pre-computed three-dimensional (3D) velocity fields for the sea area of interest and specialized particle tracking codes such as TRACMASS (Döös 1995, Blanke & Raynard 1997, de Vries & Döös 2001). Here, we prefer to use an alternative method of tracking the Lagrangian trajectories of current-transported passive tracers (below simply referred to as particles) that is implemented simultaneously with the numerical simulation (Andrejev et al. 2010). The result of the analysis of a set of particle trajectories is usually expressed in terms of various maps of the probabilities of hits in vulnerable regions or maps of the time it takes for the adverse impact to reach these regions (Andrejev et al. 2010, Soomere et al. 2011a,b). Also, the concept of the equiprobability line (the probability of the propagation of pollution from a particular point to the opposite coasts is equal) is used to characterize optimum fairways in elongated basins (Soomere et al. 2010) or, equivalently, between two vulnerable regions.

Computationally, the construction of such maps and studies of their reliability and associated uncertainties are usually very time-consuming and demanding. This has raised the question about potential simplifications of calculations involving a minimum loss of accuracy but retaining the reliability of the results. For longer time intervals it is possible to reduce the number of simulated trajectories without significant loss of accuracy of the resulting estimates (Viikmäe et al. 2010). A more generic way of reducing the computational efforts, however, is to decrease the resolution of the underlying hydrodynamic model. This appears to be feasible when the decrease in resolution does not affect the ability of the model to reproduce the mesoscale dynamics in the sea area in question (cf. Albretsen & Røed

2010). As computational costs increase rapidly with increasing 3D model resolution, such a reduction is critical in the context of the practical use of this methodology. A natural limit for such a simplification is the request that the model should, at least, be eddy-permitting. This is a very severe request in the Baltic Sea and especially in the Gulf of Finland, where the baroclinic Rossby radius of deformation is quite small, usually about 2–4 km (Alenius et al. 2003), and even smaller at the easternmost end of the Gulf, where it sometimes reaches values as small as 500 m.

The experience of several recent studies of the dynamics and hydrography of different sea areas suggests that although the instantaneous fields of simulated currents are quite different and even the statistics of currents shows substantial changes for different model resolutions (Albretsen & Røed 2010), the salinity or temperature fields can be reasonably replicated using models that poorly resolve the mesoscale dynamics. Moreover, these fields remain practically the same at different resolutions (Myrberg et al. 2010, Andrejev et al. 2010). For example, the simulations in Andrejev et al. (2010) show that the structure of the simulated current field in the Gulf of Finland may change its character abruptly when the resolution is increased from 0.5 nautical miles (nm) to 0.25 nm but that the salinity and temperature fields are almost the same as for a resolution of 1 nm (Andrejev et al. 2010).

In this paper we address the question of whether the above-mentioned maps of environmental risks (reflecting, in essence, long-term statistics of the current-driven transport constructed using large pools of Lagrangian trajectories), or at least certain of their integral features, belong to the family of those characteristics that are mostly insensitive to changes at the resolution of the underlying ocean model. The test area is the Gulf of Finland, the easternmost extension of the Baltic Sea (Figure 1). This is an elongated water body with a length of ca 400 km, a maximum width of 135 km and a mean depth of only 37 m (Soomere et al. 2008). It is a basin with extremely complicated internal dynamics (Andrejev et al. 2004a,b, Soomere et al. 2010), for which the basic idea of the use of intrinsic dynamics of water masses for the smart relocation of potentially dangerous activities was first formulated by Soomere & Quak (2007).

The gulf hosts heavy east-west cargo traffic (HELCOM 2009) and very intensive passenger traffic across it in the relatively narrow section between Tallinn and Helsinki (Parnell et al. 2008, Kurennoy et al. 2009). As the gulf is less than 80 km wide in some places and the water too shallow for marine transportation in others, there are several narrow passages where the concentration of traffic is exceptionally high. Therefore, there exists a high probability that various adverse impacts (oil or chemical pollution,

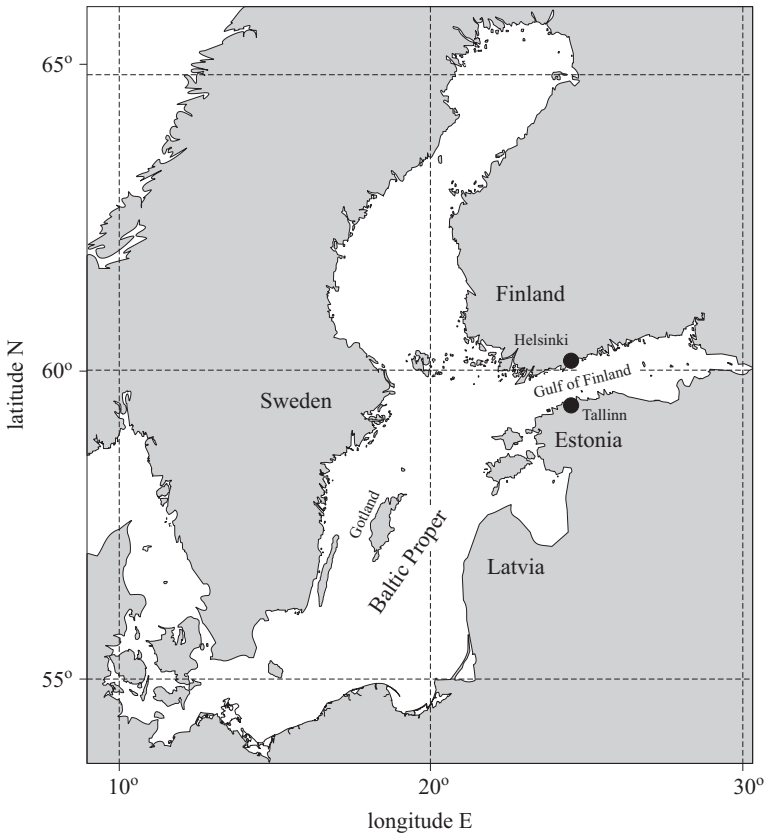

Figure 1. Map showing the location of the Baltic Sea and the Gulf of Finland

lost containers or other large floating objects, etc.) may be released along the shipping route as a result of an accident, technical problems or human error or misbehaviour. The most dangerous event from the environmental viewpoint is a large-scale oil pollution event hitting the coastal area. For this reason, we perform the analysis in terms of the problem of identifying the environmentally safest fairway along the gulf with respect to coastal oil pollution.

We construct a sequence of 2D maps characterizing ship-traffic-induced environmental risks. Based on these maps, we develop an application targeted at a selection of optimum locations for potentially dangerous activities. This is done using a range of different resolutions of the hydrodynamic model, from a barely eddy-permitting tool to its high-resolution (but otherwise identical) version. The particular goal is to identify an optimum spatial resolution for the ocean model for different applications of the entire method. We start from a horizontal resolution

of 2 nm and gradually increase the resolution down to 0.5 nm. This range of resolutions characterizes a transition from quite a poor representation of mesoscale effects in this basin to one which is expected to adequately resolve the field of mesoscale eddies at nearly every time instant and place. While the 2 nm model is, at best, an eddy-permitting model for the Gulf of Finland, the 0.5 nm model is expected to resolve most of the mesoscale eddy dynamics in this basin. Although the models in use enable the full 3D tracking of particles, for simplicity and in order to highlight the potential differences in the horizontal resolution, we lock the particles in the uppermost layer.

Section 2 gives a short overview of the basic features of the ocean model in use, describes the technology for solving the inverse problem for environmental management and briefly discusses the measures for quantifying the environmental risks. Most of the material in this section is classical and presented here only for completeness. The reader is referred to Andrejev et al. (2010), Soomere et al. (2010, 2011a,b) and Viikmäe et al. (2010) for details. The key new information is presented in sections 3–5, where we discuss in detail the dependence of the resulting maps and the optimum locations of the fairway on the spatial resolution of the ocean model. Section 6 presents a synopsis of the analysis and sketches further research needs.

2. The OAAS model and methods for trajectory analysis

The method for identifying the optimum fairway consists of four basic steps (Andrejev et al. 2010, Soomere et al. 2010, 2011a,b). The 3D dynamics of water masses in the sea area in question is simulated numerically, and the results of the simulations are used to construct Lagrangian trajectories of selected water particles. Together with a cost function, these trajectories are used to construct maps characterizing the distribution of the environmental risks associated with different offshore areas. The final step is the identification of the optimum location for fairways. An important feature of the entire approach is that the particular methods comprising each step may be addressed separately without the loss of generality for the entire procedure.

The 3D OAAS hydrodynamic model (Andrejev & Sokolov 1989, 1990) is used for modelling the Gulf of Finland's circulation properties. This time-dependent, free-surface, baroclinic model is written in z-coordinates and is based on the hydrostatic approximation. It was specifically developed for use in basins with a complicated bathymetry and hydrography, such as the Gulf of Finland, but it is obviously applicable to any water body of comparable size. The model has shown excellent performance in different

applications, from basin-scale estimates of the upwelling features in the entire Baltic Sea and mean circulation and water age of the Gulf of Finland (Andrejev et al. 2004a,b) down to the small-scale reproduction of surface buoy drift (Gästgifvars et al. 2006). The quality of the simulation of the hydrophysical fields is analysed in detail within the framework of a model intercomparison for the Gulf of Finland (Myrberg et al. 2010).

The model resolution for the Gulf of Finland was originally restricted to 1 nm in order to match the available bathymetric information for the entire Baltic Sea (Seifert et al. 2001) but has been recently increased to 0.25–0.5 nm. A detailed description of the features and approximations of the latest high-resolution version of the model is presented in Andrejev et al. (2010). In order to ensure comparability of the results with earlier studies (Andrejev et al. 2004a,b, Soomere et al. 2010), we used the simulation period of 1 May 1987–31 December 1991. The OAAS model was run for the Gulf of Finland to the west of longitude 23°27′E (Figure 2) at three different horizontal resolutions – 0.5, 1 and 2 nm – but with an otherwise identical vertical resolution (1 m) and forcing and boundary conditions.

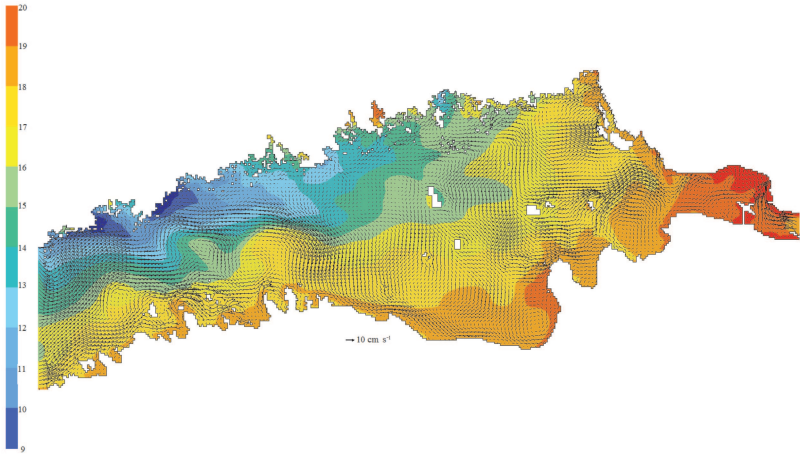

Figure 2. Map of surface velocities (vectors, every 3rd grid point represented in each direction) and sea surface temperatures (°C, colour scale) in the Gulf of Finland in a simulation at a resolution of 0.5 nm for 4 August 1987

The impact of the rest of the Baltic Sea is accounted for in the form of the relevant boundary conditions along this longitude, optionally with the sponge layer approach (see Andrejev et al. 2010 for details). The boundary conditions (salinity, temperature and sea-level elevation) were extracted at 6 hour intervals from simulations performed with the Rossby Centre coupled

ice-ocean model (RCO, Meier et al. 2003). The RCO model is based on the Bryan-Cox-Semptner primitive equation ocean model with a free surface but contains several parameterizations with a special importance for the Baltic Sea, such as a two-equation turbulence closure scheme, open boundary conditions and a sea-ice model. It was run with a horizontal resolution of 2 nm that is usually sufficient for eddy-resolving runs in the Baltic Proper (Lehmann 1995). The initial sea water temperature and salinity fields for all the OAAS model resolutions were constructed by an interpolation of the RCO data. The modelling in the Gulf of Finland started from the resting water masses and with the sea level equal to the barometric equilibrium. Owing to the realistic initial data and high-quality boundary information, the modelled fields are plausible from the very beginning of calculations and the final spin-up of the model takes ca 1–2 weeks for the surface layer dynamics.

The meteorological forcing for both the OAAS and RCO models is based on the relevant fields (atmospheric pressure, temperature, wind speed components, total precipitation, specific humidity, and total cloud cover with a temporal resolution of 3 hours) downscaled from the ERA-40 database using a regional atmosphere model covering the entire Baltic Sea at a horizontal resolution of 25 km (Samuelsson et al. 2011). River discharge is approximated in terms of monthly mean values for the period 1970–1990 (Bergström & Carlsson 1994). The salinity of river water is set to zero and its temperature equal to the ambient sea water temperature at the river mouth. This approximation (equivalent to ignoring the flux of heat and salt from the rivers) is reasonable for Baltic Sea conditions, where the salt content of river water is negligible and the difference between river and sea water temperatures is moderate. As the winters during the period of interest were rather mild and the Gulf of Finland was mostly free of ice, we have neglected ice drift and used a simple parameterization for ice formation and melting. For water temperatures below freezing point, the wind stress is decreased by a factor of 10 in order to mimic the presence of ice and the resulting tilt of the ice-covered surface. At 0°C, the heat flux through the ice is stopped as long as cooling conditions prevail. The loss of heat during ice melting is approximated by decreasing the upward-directed heat flux in the early spring by a factor of four until the sea water temperature reaches the value of +1°C.

The second key component of the method is a set of Lagrangian trajectories of water particles, which is equivalent to a set of particular solutions to the direct problem of propagation of an adverse impact. In order to create a large number of independent trajectories, the simulation interval is usually divided into shorter (optionally partially overlapping)

time windows (Soomere et al. 2010, Viikmäe et al. 2010). The necessary duration of these windows, the time lag between them and the number of trajectories considered (equivalent to the number of particles released into the water), depends essentially on the environment under scrutiny. In terms of potential oil pollution, the transport of substances released from ships to the shoreline (referred to below as a 'coastal hit') is regarded as an undesirable event. For studies of ship-caused coastal pollution and for evaluating the potential risks of ship traffic in the Gulf of Finland, the optimum length of the time window is ca 10 days, during which an appreciable number of coastal hits occurs (Viikmäe et al. 2010). The results are almost insensitive to the time lag between windows, provided the number of windows is large enough. The resulting patterns of risk characteristics are also largely insensitive to the number of particles released into each grid cell (Soomere et al. 2010, Viikmäe et al. 2010).

Based on the features discussed, we calculate the set of Lagrangian trajectories (Figure 3) as follows. The entire modelling period (1 May 1987 –31 December 1991) is divided into 170 consecutive 10-day time windows. At the beginning of each window ten particles are released into each surface grid cell. In order to specifically highlight the effect of changing spatial resolution on the results and also to make our results comparable with those in Soomere et al. (2010, 2011a,b), these particles are locked in the

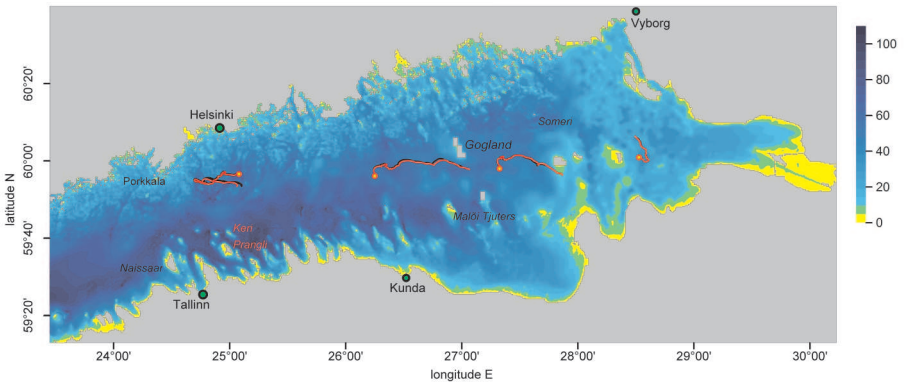

Figure 3. Examples of Lagrangian trajectories in the Gulf of Finland in summer conditions (01–10 June 1987) against the background of a high-resolution (0.5 nm) bathymetry of the Gulf of Finland. The depth scale to the right of the map is given in metres. Two particles were released into each of four points and were tracked during 10 days. The differences in the trajectories between these particles (black and red lines) due to the influence of the random component of velocity are fairly small except for the easternmost pair

uppermost layer: doing so mimics the current-induced transport of relatively light substances. The method itself allows for the full three-dimensional tracking of particles.

The dynamics of water masses in the Gulf of Finland is extremely complicated, and the resolution of even the 0.5 nm model does not perfectly resolve all the small-scale features of water motion. Therefore, sub-grid-scale processes evidently play a relatively large role in the dynamics even at the highest resolution used in this paper. The potential impact of sub-grid-scale turbulence on the spreading of initially closely located particles is usually parameterized by the addition of a random disturbance to the flow field. In order to reflect the presence of a number of mesoscale vortices in this water body, we add such a disturbance containing a strong rotational component and with a magnitude comparable to that occurring naturally in the surface layer of the Baltic Sea (Andrejev et al. 2010) on top of the transport calculated using velocity fields.

The resulting set of trajectories can be used to study a variety of properties of current-driven transport. For example, Soomere et al. (2011c) used it to investigate the properties of net and bulk transport (the length of the trajectory and the final displacement of the particle respectively) in flow systems with relatively rapidly alternating directions. In the context of the quantification of the environmental risks caused by current-induced transport an obvious choice is to estimate the probability of hitting vulnerable regions (Soomere et al. 2010, Viikmäe et al. 2010). A quantity even richer in content is the time necessary for the adverse impact to reach the vulnerable area (particle age, Engqvist et al. 2006, Soomere et al. 2011a).

Following Kokkonen et al. (2010) and Soomere et al. (2010), we choose coastal areas as examples of vulnerable regions, but unlike the latter authors, we do not distinguish specific coastal sections (like the northern and southern coast). We apply two quantities to characterize a particular offshore sea point: the probability of a coastal hit and the particle age. The relevant counters are associated with each particle released. The counter used for the calculation of probabilities is set to 1 if the particle hits any section of the coast during the 10-day time window and to 0 if this does not happen. The latter case reflects situations when the particle travels offshore during the whole time or leaves the Gulf of Finland. The other variable counts the time during which the particle is located offshore either within the Gulf of Finland or in other areas of the Baltic Sea. The maximum value of this variable is limited by the duration of the time window. Therefore, the estimate of the particle age (the average time for the coastal hit)

is apparently underestimated for areas with a low probability of coastal hits.

The cell-wise probabilities of coastal hits $P_{i,j}^{(k)}$ and particle age $A_{i,j}^{(k)}$ are calculated for each time window k (out of a total of $N = 170$ time windows) in a straightforward way as the average of the relevant values p_{mk}^{ij}, a_{mk}^{ij} over all M particles released into a particular cell (i, j):

$$P_{i,j}^{(k)} = \frac{1}{M} \sum_{m=1}^{M} p_{mk}^{ij}\,, \qquad A_{i,j}^{(k)} = \frac{1}{M} \sum_{m=1}^{M} a_{mk}^{ij}\,. \tag{1}$$

Here p_{mk}^{ij} and a_{mk}^{ij} are the values of the counters showing, respectively, whether the m-th particle released into grid cell (i, j) at the beginning of the k-th time window has reached the coast during this window and the particle age either at the instant of the first coastal hit or, alternatively, the duration of this time window if the particle remains offshore.

This procedure leads to two sets of 2D maps (with a spatial resolution equal to that of the circulation model) of the cell-wise probability of particles released into a particular cell hitting the coast (below referred to as 'probability') and the mean time (particle age) for coastal hits for particles from this cell. The first quantity is a variation of the measure of the probability of coastal hits used by Soomere et al. (2010) to identify the equiprobability line for coastal hits in the Gulf of Finland. The two variables obviously mirror each other to some extent. For example, the minimum of probability evidently occurs more or less where the particle age reaches a maximum. Consequently, the optimum fairways found on the basis of these fields should be located close to each other. The difference between them can be interpreted as a measure of the uncertainty of the entire approach (Soomere et al. 2010). Note that particle age is really much more informative. For example, it is easy to convert particle age to probability (if the age of a particle is less than the duration of the time window, a coastal hit has occurred) but it is impossible to convert the probability to age.

3. Time series of average probability and particle age

We start the analysis of the similarities and differences of the results for different model resolutions by comparing the average values of the probability $P(k) = \left\langle P_{i,j}^{(k)} \right\rangle$ and particle age $A(k) = \left\langle A_{i,j}^{(k)} \right\rangle$ over all particles released into the entire Gulf of Finland for a particular time window k. Here, the angled brackets signify the operation of taking the arithmetic mean over all L sea points in the calculation area ($L = 2270$ for the 2 nm model, $L = 8810$ for the 1 nm model and $L = 31838$ for the 0.5 nm

model (Andrejev et al. 2010)). Another pair of important quantities are the cumulative average probability $\overline{P}(n)$ for the coastal hit and the cumulative average age $\overline{A}(n)$ of all particles over the entire calculation area and for the first n time windows. They are defined in the classical way:

$$\overline{P}(n) = \frac{1}{n}\sum_{k=1}^{n} P(k), \qquad \overline{A}(n) = \frac{1}{n}\sum_{k=1}^{n} A(k). \tag{2}$$

The average probability $P(k)$ over particular time windows reveals extensive seasonal variation, from about 0.4 (mostly in calm seasons) to values very close to 1 (Figure 4). The cumulative probability $\overline{P}(n)$ reaches an asymptotic value (ca 0.67) after the first half-year of simulations and reveals only very moderate variations (ca ± 0.03) after about two years of calculations. Consequently, the integral features of this probability are apparently established within a few years, and later variations in their values are fairly minor.

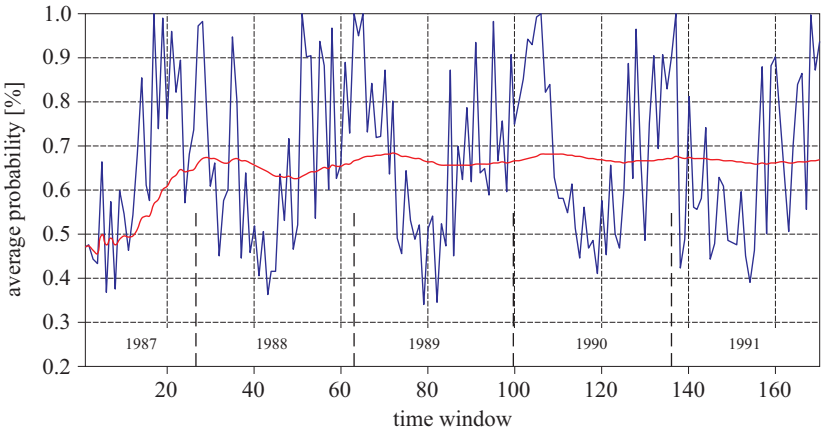

Figure 4. Mean probability $P(k)$ for particular time windows (blue) and cumulative average probability $\overline{P}(n)$ over the first n time windows (red) in simulations at a horizontal resolution of 1 nm

The temporal course of the mean particle age $A(k)$ is, as expected, largely in antiphase with the above probability and also reveals a clear seasonal cycle (Figure 5). The relative variations in the values of both quantities have almost the same range (the maximum values are about three to six times as large as the minimum ones). The largest probabilities occur roughly simultaneously with the smallest particle age during autumn and winter storms. These extremes apparently reflect very large velocities of the Ekman drift during stormy periods. The cumulative average particle age

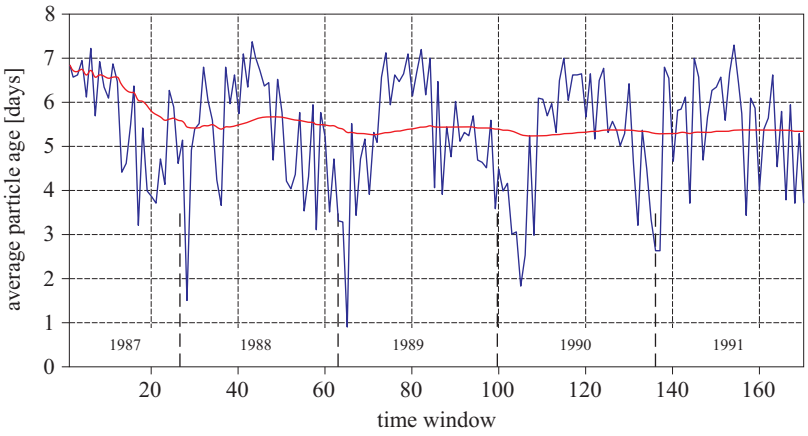

Figure 5. Mean particle age $A(k)$ for particular time windows (blue) and cumulative average particle age $\overline{A}(n)$ over the first n time windows (red) in simulations at a horizontal resolution of 1 nm

$\overline{A}(n)$ also reaches a more or less constant value of ca 5.3 days after a couple of years of simulations.

Interestingly, the temporal course of these quantities is very similar for all simulations with different horizontal resolutions (Figures 6, 7). Somewhat unexpectedly, the seasonal variation in the difference is almost missing for the probability, whereas it is quite weakly present for the particle age (Figure 7).

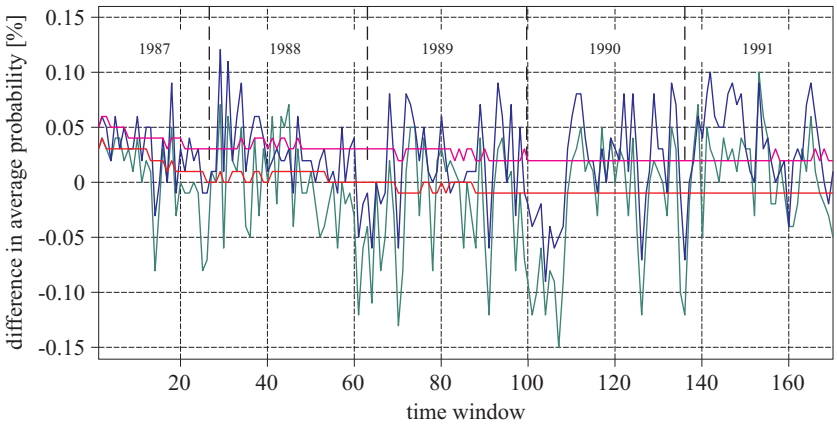

Figure 6. Difference between the mean probability $P(k)$ and the cumulative average probability $\overline{P}(n)$ calculated at different horizontal resolutions. Green and red: difference between the results of the 1 nm and 2 nm models; blue and magenta: difference between the results of the 1 nm and 0.5 nm models. The results for the 1 nm model are shown in Figure 4

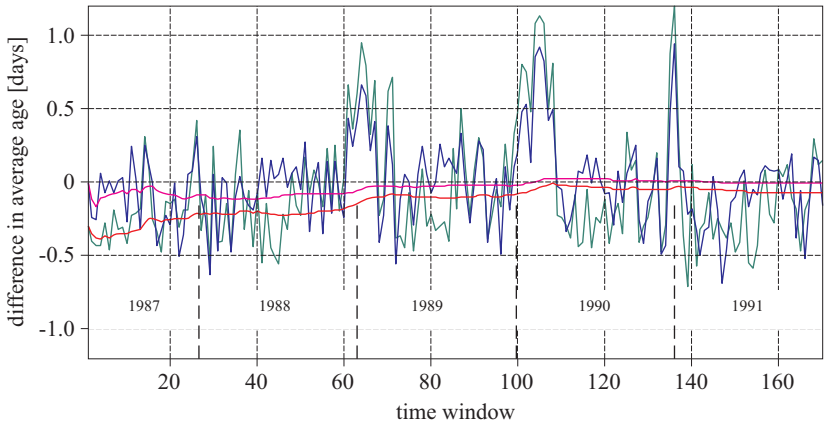

Figure 7. Difference between the mean particle age $A(k)$ and its cumulative value $\overline{A}(n)$ calculated at different horizontal resolutions. Green and red: difference between the results of the 1 nm and 2 nm models; blue and magenta: difference between the results of the 1 nm and 0.5 nm models. The results for the 1 nm model are shown in Figure 5

The small difference between the spatially averaged results obtained at different resolutions can be easily verified by treating time series $P(k)$ and $A(k)$ as sequences of random variables and applying standard statistical methods in order to characterize their match (Table 1). The time series of the mean probability and particle age, averaged over all trajectories within a time window, show a very high correlation (0.98 for the 1 nm and 0.5 nm

Table 1. Mutual statistical characteristics for the mean probability and mean age of particles calculated at 1 and 0.5 nautical mile resolution. The values are calculated using the classical relations $\overline{R} = \left(\sum R_i\right)/N$ for the mean value and $\sigma_{RR} = \sqrt{\left(\sum \left(R_i - \overline{R}\right)^2\right)/(N-1)}$ for the standard deviation for a sample of N values of the quantity R_i, $i = 1 \ldots N$, where all summations are performed over a total number $N = 170$ of time windows. The correlation coefficient is $\rho = \left[\sum \left(R_i - \overline{R}\right) \times \left(Q_i - \overline{Q}\right)\right]/[(N-1)\sigma_{RR}\sigma_{QQ}]$, the mean absolute and root-mean-square difference are estimated as $MAD = \sum |R_i - Q_i|/N$ and $RMSD = \sqrt{\sum (R_i - Q_i)^2 / N}$, respectively; bias is defined simply as $B = \overline{Q} - \overline{R}$ and spread as $S^2 = \sum \left[\left(Q_i - \overline{Q}\right) - \left(R_i - \overline{R}\right)\right]^2/(N-1)$, and Q and R may stand for A or P

	Correlation coefficient ρ	Bias B	Mean absolute deviation MAD	$RMSD$	Spread S^2
probability	0.98	−0.024	0.037	0.0021	0.0015
particle age	0.98	0.012	0.21	0.081	0.081

simulations) and small bias, mean and root-mean-square deviation, and also a very low level of spread.

Moreover, the standard deviations for these fields calculated with respect to their average values are quite close for different resolutions (Table 2). This suggests that the variations in these fields with respect to the mean values have, on average, a similar structure. This harmony suggests that the spatially averaged values of the probability and particle age are largely independent of the particular resolution (provided, of course the resolution is fine enough to reproduce the basic dynamic features of the water body in question). Therefore, the quantities in question are to some extent similar to certain scalar fields such as salinity and temperature that also are well represented by eddy-resolving models starting from a 1 nm resolution.

Table 2. Mean values and standard deviations of the time series of the probability and particle age for simulations with different resolutions

Resolution, nautical miles	Mean probability $\overline{P}$	Standard deviation of probability σ_{PP}	Mean probability over optimum fairway	Mean particle age [days] $\overline{A}$	Standard deviation of particle age σ_{AA}
2×2	0.66	0.16	0.432	5.25	1.06
1×1	0.67	0.19	0.457	5.33	1.30
0.5×0.5	0.69	0.17	0.536	5.32	1.26

4. Spatial variations in the probability of coastal hit and particle age

The above has shown that several key integral characteristics of the fields of probabilities and particle age (in particular, their cumulative values) are practically insensitive to the particular horizontal resolution of the ocean model. The impact of the resolution becomes slightly more evident in a comparison of 2D maps of these characteristics. The maps in Figures 8 and 9 are constructed by the cell-wise averaging of the probabilities of coastal hits $P_{i,j}^{(k)}$ and particle age $A_{i,j}^{(k)}$ over all $N = 170$ time windows covering the simulation period 1987–1991.

The areas with relatively large particle ages and relatively small probabilities of coastal hits are located, as expected, far from coasts and islands, and mostly coincide. The most impressive feature of these maps (Figures 8 and 9) is a strong asymmetry: the domains with the lowest probabilities (in other words, the largest particle age) are substantially shifted with respect to the domains that are located at the greatest distance

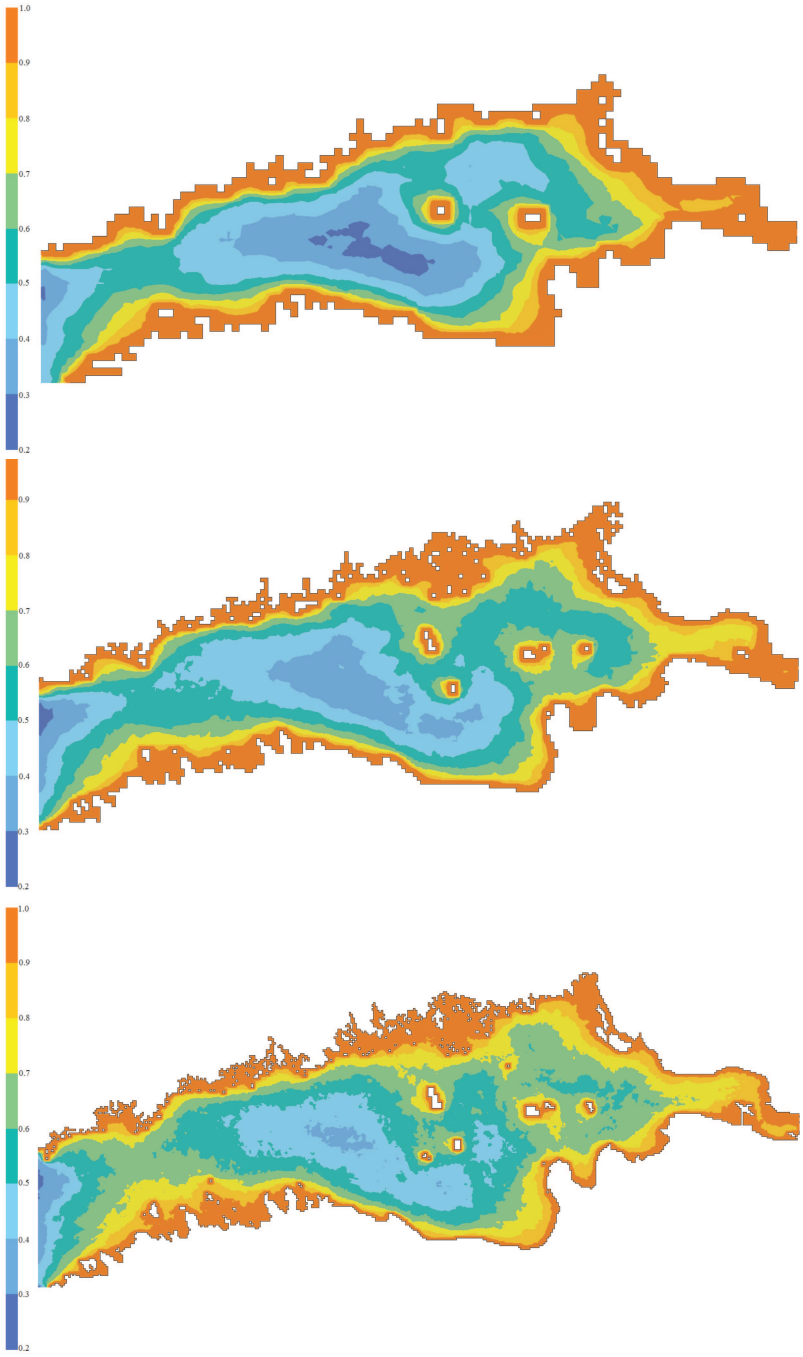

Figure 8. Probability for a coastal hit in the Gulf of Finland simulated with the use of the 2 nm (upper panel), 1 nm (middle panel) and 0.5 nm models (lower panel) for the period 1987–1991

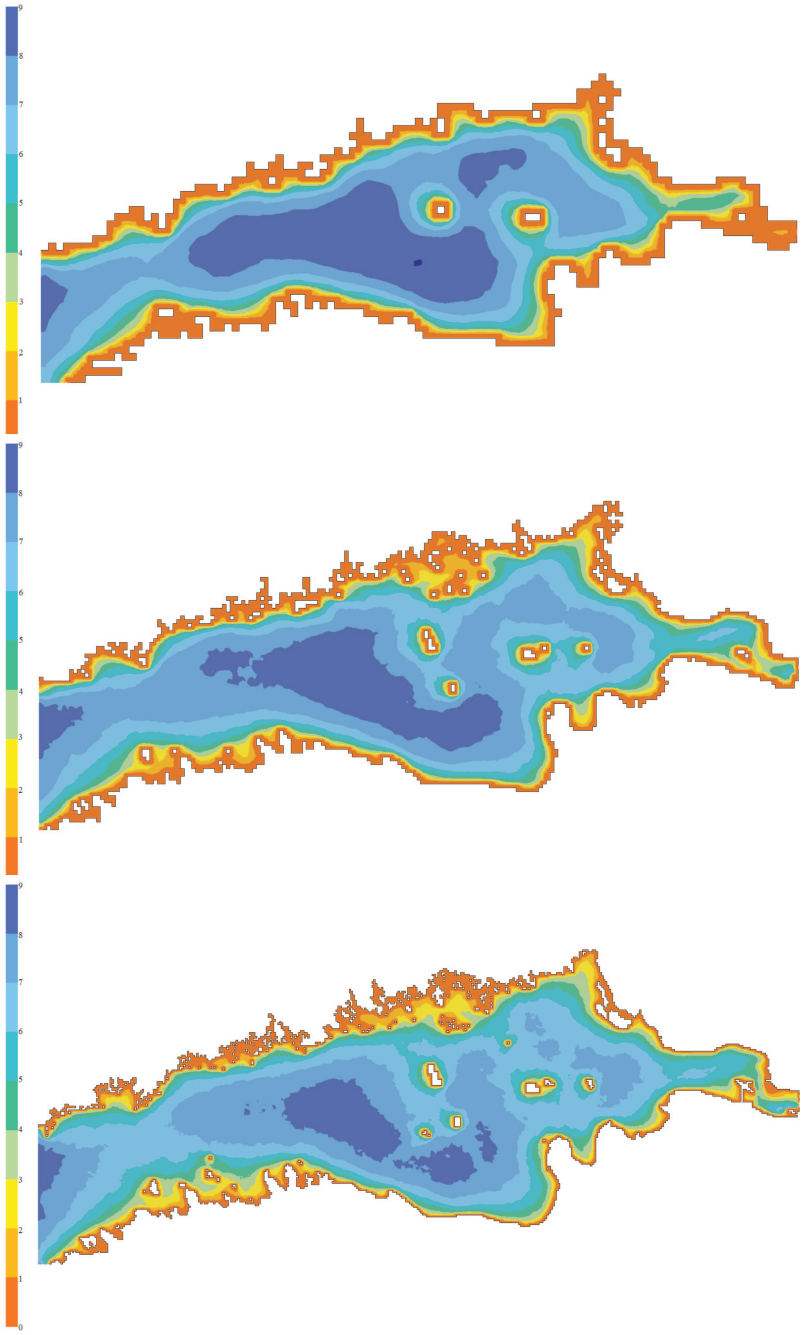

Figure 9. Particle age in the Gulf of Finland simulated with the use of the 2 nm (upper panel), 1 nm (middle panel) and 0.5 nm models (lower panel) for the period 1987–1991

from the coasts. This feature is particularly evident in the narrowest part of the gulf between Tallinn and Helsinki. In essence, this asymmetry signifies that the entire approach leads to nontrivial results for the Gulf of Finland. It is also noteworthy that the areas of minimal probability (maximal age) correspond well with sea areas hosting either a relatively intense westward mean (subsurface) transport or with domains with quasi-steady eddies (cf. Figure 11 of Andrejev et al. 2004a). This match suggests, in particular, that these quasi-steady eddies mostly reflect the overall shape of the gulf's bathymetry rather than dynamic mesoscale features. Such a 'geometric' determination of the location of a cluster of eddies may be a potential background for the similarity of the results obtained with the models at 1 nm and 0.5 nm resolution. Both models reasonably reproduce the bottom shape.

The resulting fields of probability and particle age calculated at different resolutions differ insignificantly in terms of both the qualitative appearance of the maps and the location of areas of low probabilities and high particle ages. There are only very minor differences between, for example, the relevant maps at the resolutions of 1 and 0.5 nm (Figures 8, 9). The largest differences become evident in the size of the areas of the smallest probabilities (< 0.4) and the areas of the largest particle age (> 8 days). For example, domains of very small probability or of very large particle age are larger in the calculations with the 1 nm model.

There may be several reasons for these differences in Figures 8 and 9. The change in the horizontal resolution most probably plays the greatest part in their formation: its increase evidently leads to a much better reproduction of mesoscale eddies because of the better resolution of these phenomena in general. This change is, however, inseparable from the more accurate resolution also of those features of the velocity fields in higher-resolution models that are not directly connected with the model's ability to resolve the internal Rossby radius of deformation.

Although we carefully kept the initial, forcing and boundary conditions identical for the models in use, the resulting maps implicitly depend on several side effects. The largest impact among them is obviously due to differences in the geometry of the entire domain connected with the presence of some small islands, such as Keri to the north of Prangli, Sommers (Someri) between Gogland and Vyborg, and Malyj Tjuters (Pieni Tytärsaari, also Väike Tütarsaar) to the north-east of Kunda at the 0.5 nm resolution (Figure 3). The presence of these islands and the more exact representation of other features of islands and the mainland are apparently responsible for a large part of the small-scale variations and the quite high level of noise in the fields of probability and particle age in the maps at the

0.5 nm resolution. To a certain extent these variations and noise appear to be balanced by the effects caused by the increase (from 4 to 16 times) in the total number of particles released into the system at different resolutions. In general, the accuracy of the statistical estimates (based on a larger number of trajectories) should be better for the finer models owing to the increase in both the detail of the simulations and the number of test particles. Together, the described effects seem to lead to a significant increase in the complexity of the fine structure of the resulting fields. On the other hand, their contribution apparently does not affect the average properties of the above-discussed fields calculated over five years, as the shape and location of the isolines for the relevant fields are almost the same.

5. Variations in the optimum location of the fairway

For completely isotropic and homogeneous patterns of currents the resulting distributions $P_{i,j}$ and $A_{i,j}$ should basically reflect the distance of a particular sea area from the nearest coast. However, the patterns of currents are usually essentially inhomogeneous and anisotropic (Andrejev et al. 2004a,b). This feature gives rise to an additional internal structure of these distributions. The systematic use of spatio-temporal variations in these distributions in order to minimize environmental risks is a highly nontrivial multi-dimensional optimization problem. Its particular solutions and how to estimate the potential gain from the use of a smart fairway are discussed in detail elsewhere (Soomere 2011a,b). Here, we only focus on the demonstration that the resulting solutions may be much more strongly affected by the particular horizontal resolution of the ocean model than the integral variables and 2D maps discussed above.

For elongated sea areas and a coastal hit as an undesirable event, it is reasonable to assume that the resulting probability distribution contains an elongated minimum that to some extent follows the shape of the basin. Similarly, the distribution of particle age is expected to contain an elongated maximum (Figures 8, 9). In the Gulf of Finland the majority of ships carrying the largest adverse impacts sail from the Baltic Proper along the gulf to large ports in the eastern part of the gulf (HELCOM 2009). We propose a greatly simplified algorithm for constructing an example version of the optimum fairway leading to Vyborg (Figure 3). The beginning of the fairway near Vyborg is selected manually at the closest sea point to the port where the probability is ≤ 0.9 or the age ≥ 1 day. The next fairway point is sought among the five adjacent points located in the major direction of the ship's route to the west as in Figure 10 as a point in which the minimal probability (or the maximal age of particles) of these five points occurs. The process is repeated until the westward-sailing ship reaches the Baltic

Proper. Note that the process is not symmetrical with respect to change in sailing direction and generally fails to establish the optimum fairway for ships sailing eastwards to the ports in the gulf. In essence, this procedure is a discrete variation of the method of the least steep gradient for finding crests or troughs on a 2D map of elevations. For the case where the relevant fields have exactly one minimum across the gulf, the method obviously finds this minimum and follows it.

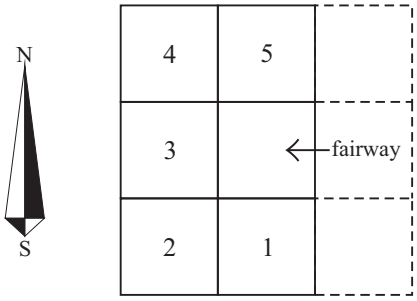

Figure 10. Scheme to illustrate the algorithm for calculating an optimum fairway. The next fairway point is chosen from among the centres of cells of the computational grid (denoted by numbers 1–5) adjacent to the instantaneous location of the ship (marked by the arrow)

As the general appearance of the distributions for the probabilities and particle age are fairly similar and the relevant maxima and minima match each other well, it is not surprising that the resulting optimum fairways (not shown) are located quite close to each other for each resolution. They almost overlap in the relatively narrow part of the gulf between Naissaar and Porkkala and in the narrow passages between the islands, for example, to the south of Gogland at different resolutions (Soomere et al. 2011a,b). Neither is it unexpected that they deviate up to 20 km from each other in the widest sections of the gulf where the relevant gradients in the underlying fields are small (Soomere et al. 2010) and where even small levels of noise may relocate the extremes by a considerable distance. Surprisingly, the two optima may also deviate considerably in the narrow area between Tallinn and Helsinki that hosts extremely heavy cargo and passenger ferry traffic.

The optimum fairways calculated using different resolutions show much more complicated patterns of mutual behaviour. For example, according to the spatial distributions of the probability for coastal hits, the fairways to Vyborg visit completely different areas of the Gulf of Finland (Figure 11). While the differences between the fairways at the 1 nm and 0.5 nm resolutions are moderate, the fairway for the 2 nm model reflects a completely different pattern of underlying dynamics, especially in the eastern Gulf of

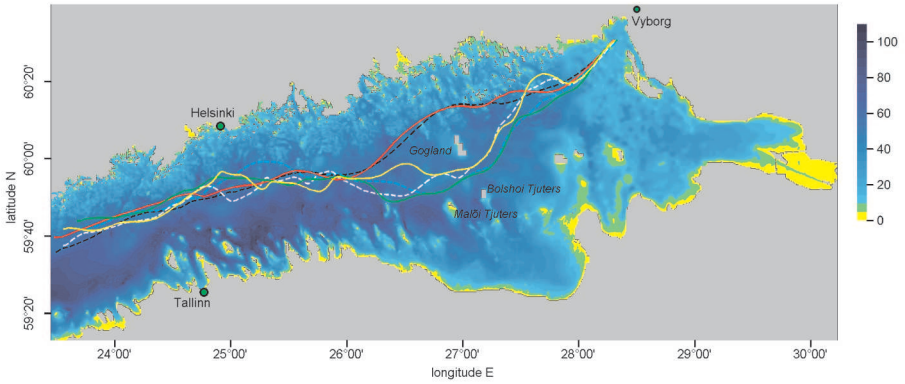

Figure 11. Optimum fairways to Vyborg according to the spatial distributions of the probability for coastal hits (solid lines) and of the particle age (dashed lines) at resolutions of 2 nm (red and black respectively), 1 nm (green and cyan) and 0.5 nm (yellow and white). The depth scale to the right of the map is given in metres

Finland. This example vividly illustrates the importance of the impact of the particular horizontal resolution on the resulting location of the optimum fairway. As mentioned above, we cannot distinguish on the basis of our simulations whether or not this difference is driven mainly by the accuracy of current simulations and/or whether the accuracy of the representation of the Finnish archipelago plays a role here.

Finally, we mention that the potential gain from the use of the optimum fairway can be roughly estimated as the difference between, for example, the mean probability of coastal hits and the average value of this probability along the optimum fairway (Table 1). Surprisingly, the gain is not directly connected with the length of the resulting fairway: the longest of the three optima in Figure 11 offers the largest gain and leads to a decrease in the relevant probability from the mean value of 0.67 to 0.46 along the fairway.

6. Discussion and conclusions

This analysis confirms that the proposed approach – using Lagrangian trajectories for quantifying the environmental risks connected with current-driven transport of adverse impacts to coastal areas – is a feasible method for the environmental management of offshore and coastal regions. It is our understanding that the largest potential for this purpose is provided by the concept of the overall average probability of hitting vulnerable regions and the accompanying quantity (particle age) characterizing the typical transport time to these regions.

Figures 4 and 5 and their analysis above suggest that the overall average probability of coastal hits and particle age converge relatively rapidly to a certain asymptotic level, although the relevant values may reveal substantial spatio-temporal variations in different sea areas and/or in different years and seasons. The discovered rapid convergence of both these quantities suggests that they can be used to characterize certain intrinsic combinations of the geometry of the basin and internal current structure: namely, the overall probability of coastal hits (for the chosen length of time window) implicitly represents the overall vulnerability of the sea area in question with respect to coastal pollution. Furthermore, the (spatial) standard deviation of this probability implicitly indicates the level of its variation across the water body and thus also the potential gain from the smart positioning of dangerous activities for the particular sea area. The average particle age is a complementary measure of the typical response time provided for the reaction to an accident. To some extent these measures are obviously characterized by the size of the water body: it is heuristically clear that very large basins correspond to small values of $\overline{P}(n)$ and large values of $\overline{A}(n)$. The above analysis, however, proves that they also implicitly characterize certain properties of current-driven surface transport that cannot be extracted directly from classical Eulerian velocity fields (cf. Soomere et al. 2011c). These properties, especially the probabilities and time scales of pollution transport from open areas of the water body to coastal regions evidently differ considerably, for example, in tide-dominated and microtidal basins of similar size. It is also natural to expect that basins hosting mostly jet-like currents will differ in this sense from regions with predominantly eddy-like mesoscale dynamics.

Another interesting feature is that the asymptotic values for the cumulative probability of coastal hits $\overline{P} \approx \lim_{n\to\infty} \overline{P}(n)$ and particle age $\overline{A} \approx \lim_{n\to\infty} \overline{A}(n)$ show very limited dependence on the resolution of the underlying hydrodynamic models. In particular, they proved to be very close to each other for the 1 nm and 0.5 nm models (Table 2). This feature shows that in some sense the 1 nm model reproduces the statistical properties of current-driven transport in the Gulf of Finland quite well. This result is not completely unexpected but is nevertheless interesting. A probable reason is that the averaging procedure of short-term transport features (but over time intervals exceeding the typical turnover time of mesoscale eddies) over the 5-year time interval filters out many short-term features of the circulation. This filtering apparently affects the results of simulations that satisfactorily capture the mesoscale features to an almost equal extent. Therefore, it is likely that many aspects of potential risks to ship traffic and/or other offshore activities in the Gulf of Finland, calculated

at a 0.5 nm (or finer) resolution, will have almost the same values as those obtained using results based on a resolution of 1 nm. This feature also suggests that many aspects of the mean circulation of the Gulf of Finland (Andrejev et al. 2004a), including those reflecting the combined effects of the prevailing south-westerly winds, the general structure of the density field, the bottom topography and the coastal shape of the gulf can be adequately calculated using a hydrodynamic model with a horizontal resolution of 1 nm.

The further example with fairway locations, however, indicates that the impact of the model resolution (and corresponding changes in the accuracy of the representation of both bathymetry and details of current patterns) becomes clearly evident in attempts to construct practical tools for decision-making about the optimum positioning of potentially dangerous activities and/or fairways. Further research is obviously necessary in order to create adequate quantification measures of the potential gain accruing from using the optimum fairway and to understand the robustness of this gain with respect to variations of such an optimum.

The key development in this light is the understanding that hydrodynamic models with a relatively low resolution (but at least eddy-permitting) may be effectively used to make the basic check whether or not any gain (in terms of a decrease in environmental risks) is possible from the smart positioning of dangerous activities in a particular sea region. This means in practice that the computing time for exercises of this type can be reduced considerably. Further, the acceptable match of optimum fairways for the 1 nm and 0.5 nm models indicates that the resulting maps of environmental risks and especially the quantities based on the relevant information are only reliable when the model is eddy-resolving. For the Gulf of Finland a resolution of 1 nm and a simulation time of a few years could be accepted as a threshold for models used for this purpose.

Acknowledgements

We are deeply grateful to Markus Meier and Anders Höglund, who provided the RCO model data and meteorological forcing within the framework of the BONUS+ BalticWay cooperation.

References

Albretsen J., Røed L. P., 2010, *Decadal simulations of mesoscale structures in the northern North Sea/Skagerrak using two ocean models*, Ocean Dynam., 60 (4), 933–955.

Alenius P., Nekrasov A., Myrberg K., 2003, *Variability of the baroclinic Rossby radius in the Gulf of Finland*, Cont. Shelf Res., 23 (6), 563–573.

Andrejev O., Myrberg K., Alenius P., Lundberg P. A., 2004a, *Mean circulation and water exchange in the Gulf of Finland – a study based on three-dimensional modelling*, Boreal Environ. Res., 9 (1), 1–16.

Andrejev O., Myrberg K., Lundberg P. A., 2004b, *Age and renewal time of water masses in a semi-enclosed basin – application to the Gulf of Finland*, Tellus A, 56 (5), 548–558.

Andrejev O., Sokolov A., 1989, *Numerical modelling of the water dynamics and passive pollutant transport in the Neva inlet*, Meteorol. Hydrol., 12, 75–85, (in Russian).

Andrejev O., Sokolov A., 1990, *3D baroclinic hydrodynamic model and its applications to Skagerrak circulation modelling*, Proc. 17th Conf. Baltic Oceanogr., Norrköping, Sweden, 38–46.

Andrejev O., Sokolov A., Soomere T., Värv R., Viikmäe B., 2010, *The use of high-resolution bathymetry for circulation modelling in the Gulf of Finland*, Estonian J. Eng., 16 (3), 187–210.

Bergström S., Carlsson B., 1994, *River runoff to the Baltic Sea: 1950–1990*, Ambio, 23 (4–5), 280–287.

Blanke B., Raynard S., 1997, *Kinematics of the Pacific Equatorial Undercurrent: an Eulerian and Lagrangian approach from GCM results*, J. Phys. Oceanogr., 27 (6), 1038–1053.

de Vries P., Döös K., 2001, *Calculating Lagrangian trajectories using time-dependent velocity fields*, J. Atmos. Ocean. Tech., 18 (6), 1092–1101.

Döös K., 1995, *Inter-ocean exchange of water masses*, J. Geophys. Res.–Oceans, 100 (C7), 13 499–13 514.

Eide M. S., Endresen Ø., Brett P. O., Ervik J. L., Røang K., 2007, *Intelligent ship traffic monitoring for oil spill prevention: risk based decision support building on AIS*, Mar. Pollut. Bull., 54 (2), 145–148.

Engqvist A., Döös K., Andrejev O., 2006, *Modeling water exchange and contaminant transport through a Baltic coastal region*, Ambio, 35 (6), 435–447.

Gästgifvars M., Lauri H., Sarkanen A.-K., Myrberg K., Andrejev O., Ambjörn C., 2006, *Modelling surface drifting of buoys during a rapidly-moving weather front in the Gulf of Finland, Baltic Sea*, Estuar. Coast. Shelf Sci., 70 (4), 567–576.

Havens H., Luther M. E., Meyers S. D., Heil C. A., 2010, *Lagrangian particle tracking of a toxic dinoflagellate bloom within the Tampa Bay estuary*, Mar. Pollut. Bull., 60 (12), 2233–2241.

HELCOM, 2009, *Ensuring safe shipping in the Baltic*, M. Stankiewicz & N. Vlasov (eds.), Helsinki Comm., Helsinki, 18 pp.

Kachel M. J., 2008, *Particularly sensitive sea areas*, Hamburg Stud. Marit. Aff. Vol. 13, Springer, Berlin, 376 pp.

Kokkonen T., Ihaksi T., Jolma A., Kuikka S., 2010, *Dynamic mapping of nature values to support prioritization of coastal oil combating*, Environ. Modell. Softw., 25 (2), 248–257.

Kurennoy D., Soomere T., Parnell K. E., 2009, *Variability in the properties of wakes generated by high-speed ferries*, J. Coastal Res., 56 (Spec. Iss.), 519–523.

Lehmann A., 1995, *A three-dimensional baroclinic eddy-resolving model of the Baltic Sea*, Tellus A, 47 (5), 1013–1031.

Lehmann M. P., Sørgård E., 2000, *Consequence model for ship accidents*, ESREL 2000, SARS and SRA-Europe Annual Conf. 17 May 2000, Edinburgh, UK.

Leppäranta M., Myrberg K., 2009, *Physical oceanography of the Baltic Sea*, Springer Praxis, Berlin, Heidelberg, New York, 378 pp.

Meier H. E. M., Döscher R., Faxén T., 2003, *A multiprocessor coupled ice-ocean model for the Baltic Sea: application to salt inflow*, J. Geophys. Res., 108 (C8), 3273, doi: 10.1029/2000JC000521.

Myrberg K., Ryabchenko V., Isaev A., Vankevich R., Andrejev O., Bendtsen J., Erichsen A., Funkquist L., Inkala A., Neelov I., Rasmus K., Rodriguez Medina M., Raudsepp U., Passenko J., Söderkvist J., Sokolov A., Kuosa H., Anderson T. R., Lehmann A., Skogen M. D., 2010, *Validation of three-dimensional hydrodynamic models in the Gulf of Finland based on a statistical analysis of a six-model ensemble*, Boreal Environ. Res., 15 (5), 453–479.

Parnell K. E., Delpeche N., Didenkulova I., Dolphin T., Erm A., Kask A., Kelpšaitė L., Kurennoy D., Quak E., Räämet A., Soomere T., Terentjeva A., Torsvik T., Zaitseva-Pärnaste I., 2008, *Far-field vessel wakes in Tallinn Bay*, Estonian J. Eng., 14 (4), 273–302.

Samuelsson P., Jones C. G., Willén U., Ullerstig A., Gollvik S., Hansson U., Jansson C., Kjellström E., Nikulin G., Wyser K., 2011, *The Rossby Centre Regional Climate Model RCA3: model description and performance*, Tellus A, 63 (1), 4–23.

Seifert T., Tauber F., Kayser B., 2001, *A high resolution spherical grid topography of the Baltic Sea*, Baltic Sea Science Congress, Stockholm 25–29 November 2001, Poster No. 147, Abstr. Vol., 2nd edn., [http://www.io-warnemuende.de/iowtopo].

Soomere T., Andrejev O., Sokolov A., Myrberg K., 2011a, *The use of Lagrangian trajectories for identification the environmentally safe fairway*, Mar. Pollut. Bull., 63, doi: 10.1016/j.marpolbul.2011.04.041.

Soomere T., Berezovski M., Quak E., Viikmäe B., 2011b, *Modeling environmentally friendly fairways in elongated basins using Lagrangian trajectories: a case study for the Gulf of Finland, the Baltic Sea*, Ocean Dynam., 61, doi: 10.1007/s10236-011-0439-y.

Soomere T., Delpeche N., Viikmäe B., Quak E., Meier H. E. M., Döös K., 2011c, *Patterns of current-induced transport in the surface layer of the Gulf of Finland*, Boreal Environ. Res., 16 (Suppl. A), 49–63.

Soomere T., Myrberg K., Leppäranta M., Nekrasov A., 2008, *The progress in knowledge of physical oceanography of the Gulf of Finland: a review for 1997 –2007*, Oceanologia, 50 (3), 287–362.

Soomere T., Quak E., 2007, *On the potential of reducing coastal pollution by a proper choice of the fairway*, J. Coastal Res., 50 (Spec. Iss.), 678–682.

Soomere T., Viikmäe B., Delpeche N., Myrberg K., 2010, *Towards identification of areas of reduced risk in the Gulf of Finland, the Baltic Sea*, Proc. Estonian Acad. Sci., 59 (2), 156–165.

Viikmäe B., Soomere T., Viidebaum M., Berezovski A., 2010, *Temporal scales for transport patterns in the Gulf of Finland*, Estonian J. Eng., 16 (3), 211–227.